J. Plasma Physics (1998), *vol.* 59, *part* 1, *pp.* 39–55. Printed in the United Kingdom

© 1998 Cambridge University Press

Magneto-optical Kerr effect for a dissipative plasma

STEPHAN C. BUCHERT

Institut für Geophysik und Meteorologie, Technische Universität Braunscheig, Mendelssohnstrasse 3, D-38106 Braunschweig, Germany

(Received 27 March 1996 and in revised form 20 January 1997)

Ion collisions in plasmas cause damping of hydromagnetic modes, but also a strong Hall effect if the collision time is of the same order as the gyroperiod. This is known to be very marked in the E region of the Earth's ionosphere, but should also occur in other partially ionized space and laboratory plasmas. In this work dynamic effects of such Hall currents are investigated theoretically. The linear modes that are obtained are, for sufficiently large scales, distinctly different from ordinary damped Alfvén modes, and similar to whistler waves even when the dynamic time scale is much longer than the ion gyroperiod. The dynamics of the coupling between planetary ionospheres and magnetospheric plasmas may be viewed as a reflection of Alfvén waves at a sharp boundary. By applying the results of the linear mode analysis, it is shown that the usually employed reflection coefficient needs to be replaced by a reflection tensor for large-scale waves due to self-induction of ionospheric Hall currents. This is similar to the magneto-optical Kerr effect, which is well-known in solid state physics. In the Earth's ionosphere, variations from incident torsional modes over periods as long as several minutes, which have been observed to occur over scales of a few thousand kilometres, are predicted to cause the generation of substantial eddy electric fields and compressional flows. Consequences for the energy exchange between ionosphere and magnetosphere and possibilities to observe the effect are discussed.

1. Introduction

Classical magneto-optical effects are known to occur in metals, semiconductors and plasmas. They are related to the Hall effect, which was discovered as a steady-state phenomenon. For a conductor of finite geometrical extension across the current flow and a static magnetic field that is applied perpendicular to the flow, an electric field across the conductor can be observed. The assumption of balance between Coulomb and Lorentz forces yields for metals the simple result

$$R_H = \frac{E_y}{j_x B_z} = -\frac{1}{n_e e} \tag{1.1}$$

for the Hall coefficient R_H, where n_e is the electron density. Ion collisions also cause a Hall effect (Chapman and Cowling 1939). This is very marked in the E region of the Earth's ionosphere, where the collision time roughly matches the gyroperiod of the ions in the geomagnetic field. The equivalent of the stationary Hall effect in solid state physics is realized at the magnetic equator of the Earth,

https://doi.org/10.1017/S0022377897006223 Published online by Cambridge University Press

leading to a vertical Hall field E_y, which, however, has not yet been observed directly. Magnetic field measurements at the ground provide indirect evidence for the equatorial electrojet driven by the atmospheric dynamo. E_y drives a secondary Hall current parallel to the primary current flow. The total current in x as a function of the applied electric field E_x is given by $j_x = \sigma_C E_x$, with the so-called Cowling conductivity

$$\sigma_C = \sigma_P + \frac{\sigma_H^2}{\sigma_P}. \tag{1.2}$$

σ_P and σ_H are the Pedersen and Hall conductivities respectively, and the local tensor relation between current and electric field (Ohm's law) is

$$\mathbf{j} = \begin{pmatrix} \sigma_p & -\sigma_H & 0 \\ \sigma_H & \sigma_P & 0 \\ 0 & 0 & \sigma_\parallel \end{pmatrix} \cdot \mathbf{E}. \tag{1.3}$$

Using the formulae (2.24) and (2.25) given in Sec. 2 for $\sigma_{P,H}$, $R_H = -1/n_e e$ is obtained for the Cowling channel as well, although, in contrast to a condensed medium, in a plasma the positively charged ions are also mobile.

In dynamic situations alternating Hall currents are produced. The well-known ion (electron) whistler where the real frequency is of the same order as the ion (electron) gyrofrequency is an example. However, also at other frequencies self-induction of transverse currents can be expected. The dynamics of such currents seem not to have been discussed in the plasma physics literature, but recently Papadopoulos *et al.* (1994) have made a similar point to that which will be made here in Sec. 2, where a linear mode analysis of low-frequency waves in a plasma with a Hall effect will be presented in a form that is convenient for the subsequent discussion of wave reflection.

In the ionosphere, time-varying Hall currents are produced by the atmospheric dynamo, and by Alfvén waves incident from space – the latter primarily at high latitudes in the aurora zones. Below the ionosphere, the conductivities drop to very small values, effectively prohibiting further propagation of Alfvén waves into the atmosphere. At low frequencies the wavelengths become much larger than the vertical atmospheric scales. Then the concept of wave reflection and transmission is appropriate. The propagation of Alfvén waves in a dissipative plasma was considered in a pioneering work by Dungey (1962), and the reflection from an ionosphere/atmosphere by Scholer (1970), neglecting Hall currents. A Fresnel type of reflection coefficient depending on the ionospheric Pedersen conductance and the magnetospheric wave impedance was obtained. This reflection coefficient has been rederived and used extensively in connection with magnetic pulsations and field-line resonances (Glassmeier 1995), is the basis for boundary conditions in numerical electrodynamic simulations (e.g. by Kan *et al.* 1991), and has been carried over to other planetary magnetosphere systems such as the 'standard ionospheric interaction model' (Prange *et al.* 1996).

In Sec. 3 the Alfvén-wave reflection is generalized to include the dynamics of a Hall effect. One of the results is the change in the polarization between incident and reflected waves, well-known in solid state physics as the magneto-optical Kerr effect (Reim and Schoenes 1990) and providing the title to this

https://doi.org/10.1017/S0022377897006223 Published online by Cambridge University Press

work. There is also a Kerr effect associated with an applied background electric field, which is not considered here.

2. Dispersion relation for dissipative Alfvén waves

Neglecting the displacement current, the wave equation obtained from Ampère's and Faraday's laws by eliminating the magnetic field is

$$k^2\mathbf{E}-(\mathbf{k}\cdot\mathbf{E})\,\mathbf{k}=i\mu_0\,\omega\mathbf{j}. \tag{2.1}$$

A harmonic variation of $\mathbf{E}$ and $\mathbf{j}$ in space and time proportional to $\exp[i(\mathbf{k}\cdot\mathbf{r}-\omega t)]$ is assumed. This equation can be closed using the local tensor Ohm's law (1.3), where the z axis of the coordinate system is parallel to the static magnetic field. The conductivity tensor is assumed to be homogeneous in real space and time. In particular, the influence of a transverse-wave magnetic field is neglected.

The analysis of linear hydromagnetic waves is accomplished by writing down the generalized, frequency-dependent conductivity tensor (or equivalently the relative dielectric tensor $\boldsymbol{\varepsilon}=\mathbf{1}+i\boldsymbol{\sigma}/\epsilon_0\,\omega$), as has been done by Stix (1962) and, including ion– and electron–neutral collisions, in the review by Holter and Kildal (1973) for a cold plasma. A wealth of modes is contained in such a description. Deeper insight into the properties of particular modes is only gained by restricting the ranges of frequencies and wavenumbers. Here we shall specialize to low-frequency waves, $\omega\ll\Omega_i$, where Ω_i is the ion gyrofrequency, but include a Hall current due to ion–neutral collisions.

Using linearized equations for the conservation of mass and momentum, neglecting pressure gradients (cold-plasma approximation) and forces other than inertia, friction with a stationary neutral background gas, and Coulomb and Lorentz forces, the conductivities for a plasma of ions and electrons can be evaluated as

$$\sigma_P=-in_e\,e^2\left(\frac{\omega+i\nu_i}{m_i[\Omega_i^2-(\omega+i\nu_i)^2]}+\frac{\omega+i\nu_e}{m_e[\Omega_e^2-(\omega+i\nu_e)^2]}\right), \tag{2.2}$$

$$\sigma_H=-n_e\,e^2\left(\frac{\Omega_i}{m_i[\Omega_i^2-(\omega+i\nu_i)^2]}-\frac{\Omega_e}{m_e[\Omega_e^2-(\omega+i\nu_e)^2]}\right), \tag{2.3}$$

$$\sigma_\parallel=+in_e\,e^2\left(\frac{1}{m_i(\omega+i\nu_i)}+\frac{1}{m_e(\omega+i\nu_e)}\right), \tag{2.4}$$

where $\nu_{i,e}$ are the collision frequencies of ions and electrons with the neutrals, and $\Omega_{i,e}$ are the respective gyrofrequencies $eB/m_{i,e}$. In literature dealing with space plasma, these formulae are frequently given for $\omega=0$. Then the conductivities are real quantities. We retain here the notation σ_P, σ_H and $\sigma_\parallel$ also for the frequency-dependent case, when in general they are complex. It is well known that, in the absence of ion collisions, the ordinary linear torsional and compressional Alfvén modes are described when setting $E_\parallel=0$ and

$$\sigma_P\approx-i\frac{\omega}{\mu_0\,v_A^2},\qquad v_A^2=\frac{B^2}{\mu_0\,n_e\,m_i}, \tag{2.5}$$

$$0\approx\sigma_H\ll\sigma_P, \tag{2.6}$$

https://doi.org/10.1017/S0022377897006223 Published online by Cambridge University Press

where v_A is the Alfvén velocity. In this limit, the P in σ_P may rather stand for 'polarization', because the transverse currents of ideal Alfvén waves are polarization currents. Inertial effects due to field-aligned electron motion produce corrections of the order of $k_\perp c/\omega_{pe}$, where ω_{pe} is the electron plasma frequency, and a field $E_\parallel \neq 0$ is obtained (Hasegawa and Uberoi 1982). This is significant only at small perpendicular wavelengths. We can expect significant effects due to self-induction mainly for large wavelengths, and we therefore start off with the assumption that $E_\parallel = 0$. In the Earth's ionosphere the sound velocity is much less than v_A, and thermal effects (including the kinetic Alfvén mode) will be neglected. For hot plasmas this will of course need to be reconsidered.

In Fig. 1 the fields and currents of an Alfvén wave in a plasma without and with a Hall effect are qualitatively compared for a special, 'coaxial-cable'-like geometry. Similarly to an ion whistler (or ion cyclotron) mode, the 'Hall–Alfvén mode' always has both torsional and compressional components. However, the phase relations between these components will be different from the dissipationless cyclotron modes, which is of course not obvious in the figure. It may be noted that the Pedersen current $\mathbf{j}_{P,i}$, which is driven by the induction field, is a dissipative load everywhere in space and time. How is the energy supplied to it? $\mathbf{j}_{H,i}$, also driven by the induction field, is closed via field-aligned currents, and thus a Poynting flux (which is not drawn) along $\mathbf{B}$ is then added or taken away via this Hall current, depending on the phase relation between $\mathbf{j}_{H,i}$ and $\mathbf{E}_A$. On average, an additional Poynting flux in z disappears via the Hall current, which must then become dissipated in the Pedersen eddy currents.

Motivated by this figure, $\mathbf{E} = \mathbf{E}_\perp$ as well as $\mathbf{j}_\perp$ are decomposed into source-free and irrotational vector fields according to the Helmholtz theorem for two dimensions:

$$\mathbf{j} = \mathbf{j}_{\mathrm{sf}} + \mathbf{j}_{\mathrm{irr}} + \mathbf{j}_\parallel, \tag{2.7}$$

$$\mathbf{E} = \mathbf{E}_A + \mathbf{E}_C, \tag{2.8}$$

where $\mathbf{E}_A$ is the wave electric field of a torsional Alfvén mode and $\mathbf{E}_C$ is the field induced by compressional magnetic variations along the z axis.

The z component of (2.1) is

$$-(\mathbf{k}_\perp \cdot \mathbf{E}_A)\, k_z = i\mu_0 \omega \mathbf{j}_\parallel. \tag{2.9}$$

Less trivially, the remaining vector equation in two dimensions has source-free and irrotational parts, which must both be fulfilled separately:

$$k^2 \mathbf{E}_C = i\mu_0 \omega \mathbf{j}_{\mathrm{sf}}, \tag{2.10}$$

$$k^2 \mathbf{E}_A - (\mathbf{k}_\perp \cdot \mathbf{E}_A)\, \mathbf{k}_\perp = i\mu_0 \omega \mathbf{j}_{\mathrm{irr}}. \tag{2.11}$$

Because we assume that $E_\parallel = 0$, Ohm's law is not used for the z component of (2.1), but for the transverse directions. Decomposition gives

$$\mathbf{j}_{\mathrm{sf}} = \sigma_P \mathbf{E}_C + \sigma_H \hat{\mathbf{z}} \times \mathbf{E}_A, \tag{2.12}$$

$$\mathbf{j}_{\mathrm{irr}} = \sigma_P \mathbf{E}_A + \sigma_H \hat{\mathbf{z}} \times \mathbf{E}_C. \tag{2.13}$$

A relation between $\mathbf{E}_C$ and $\mathbf{E}_A$ is obtained by inserting (2.12) into the source-free equation (2.10):

$$\mathbf{E}_C = -\frac{\sigma_H}{\sigma_P} \frac{y}{i+y} \hat{\mathbf{z}} \times \mathbf{E}_A, \tag{2.14}$$

https://doi.org/10.1017/S0022377897006223 Published online by Cambridge University Press

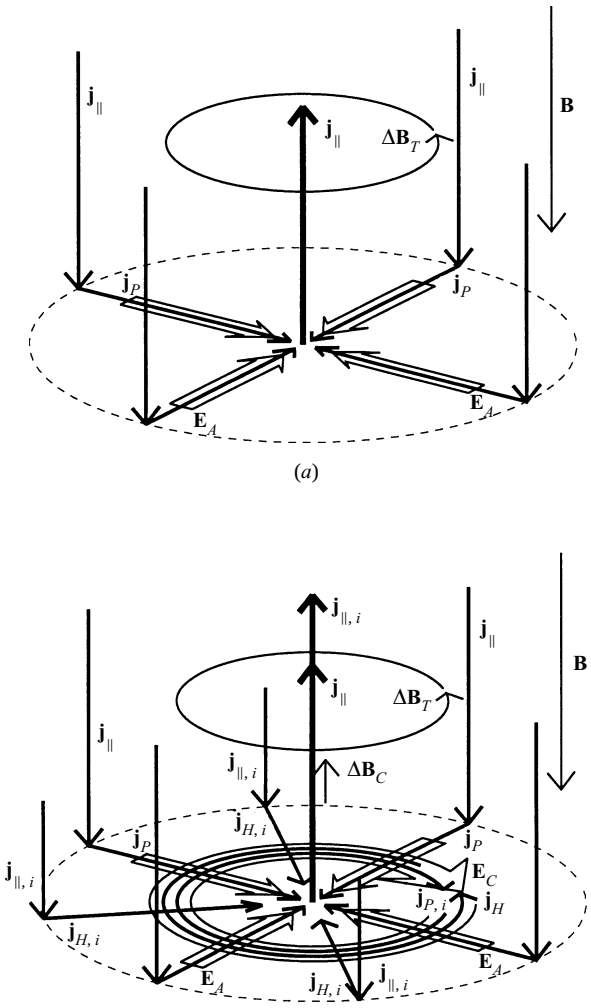


Figure 1. Snapshot of currents (solid arrows) and electric fields (outlined arrows) in a torsional mode in the absence of Hall currents (*a*), and in a coupled torsional/compressional mode with Hall currents (*b*). The arrows represent continuous vector fields of a 'coaxial-cable'-like wave structure. In (*b*) the phase with increasing $\mathbf{E}_A$, $\mathbf{j}_P$ and $\mathbf{j}_H$ is shown. $\mathbf{E}_C$ opposes the change in $\mathbf{j}_H$, thus driving the induced currents $\mathbf{j}_{P,i}$, $\mathbf{j}_{H,i}$ and $\mathbf{j}_{\parallel,i}$.

where $y = \mu_0 \omega / k^2 \sigma_P$ is a dimensionless parameter. The currents written as functions of $\mathbf{E}_A$ are

$$\mathbf{j}_{\mathrm{sf}} = -\sigma_H \frac{i}{i+y} \hat{\mathbf{z}} \times \mathbf{E}_A, \tag{2.15}$$

$$\mathbf{j}_{\mathrm{irr}} = \left(\sigma_P + \frac{\sigma_H^2}{\sigma_P} \frac{y}{i+y} \right) \mathbf{E}_A. \tag{2.16}$$

The factor inside the parentheses in (2.16), a conductivity, approaches σ_C for $|y| \gg 1$ because for very large-scale waves and/or high frequencies the phase lag of the induced field $\mathbf{E}_C$ becomes very small, and thus it can play a similar role as

https://doi.org/10.1017/S0022377897006223 Published online by Cambridge University Press

the Hall polarization field in the steady state. In general, however, complex relations between Helmholtz-decomposed currents and electric field exist, which, when inverse Fourier-transformed, are non-local in both space and time. But it should be noted that the transverse components of the local Ohm's law (1.3) for the *total* current and electric field contained in (2.12)–(2.16) can easily be recovered from them.

The irrotational vector equation (2.16) can now be closed with the intermediate result

$$\left[k^2 - i\mu_0\omega\left(\sigma_P + \frac{\sigma_H^2}{\sigma_P}\frac{y}{i+y}\right)\right]\left[k_z^2 - i\mu_0\omega\left(\sigma_P + \frac{\sigma_H^2}{\sigma_P}\frac{y}{i+y}\right)\right]\mathbf{E}_A = 0. \tag{2.17}$$

Setting the expressions in the square brackets equal to zero yields the desired dispersion relations. The first gives right and left circularly polarized waves that do not carry any field-aligned current ($\mathbf{k}_\perp = 0$):

$$k^2 = k_z^2 = \mu_0\omega(i\sigma_P \pm \sigma_H), \tag{2.18}$$

$$\mathbf{E}_C = \pm i\hat{\mathbf{z}} \times \mathbf{E}_A. \tag{2.19}$$

For arbitrary directions of propagation only the second bracket in (2.17) is applicable:

$$k^2 = i\mu_0\omega\sigma_P + \tfrac{1}{2}k_\perp^2\,[1 \pm (1+4y_H^2)^{1/2}] \tag{2.20}$$

is obtained, with $y_H = \mu_0\omega/k_\perp^2\,\sigma_H$. The elliptical polarizations of these characteristic wave modes are

$$\mathbf{E}_C = \pm i\frac{2y_H}{1 \pm (1+4y_H^2)^{1/2}}\hat{\mathbf{z}} \times \mathbf{E}_A, \tag{2.21}$$

and the currents are

$$\mathbf{j}_{\mathrm{sf}} = \left(\sigma_H + i\sigma_P\frac{2y_H}{1 \pm (1+4y_H^2)^{1/2}}\right)\hat{\mathbf{z}} \times \mathbf{E}_A, \tag{2.22}$$

$$\mathbf{j}_{\mathrm{irr}} = \left(\sigma_P - i\sigma_H\frac{2y_H}{1 \pm (1+4y_H^2)^{1/2}}\right)\mathbf{E}_A. \tag{2.23}$$

In the limit as $\mathbf{k}_\perp \to 0$, (2.20) and (2.21) of course become identical to (2.18) and (2.19).

If frequency-dependent complex conductivities are inserted, the relations (2.20)–(2.23) describe the dispersion and polarization of the whistler as well as the hydro-magnetic modes (but not the above-mentioned inertial Alfvén wave with $E_\parallel \neq 0$, kinetic modes, and high-frequency modes where the displacement current is important). We are interested in the low-frequency case with dissipation when $\omega \ll \Omega_i$, but $\nu_i \approx \Omega_i$, which is the case for example in the ionospheric E region. The real part of σ_P is much larger than the imaginary part, which is analogous to the 'good-conductor' limit of the normal skin effect for electromagnetic waves. Without the Hall effect, the well-known skin depth $\delta = 1/\Im(k_z) = (2/\mu_0\omega\sigma_P)^{1/2}$ is obtained.

https://doi.org/10.1017/S0022377897006223 Published online by Cambridge University Press

However, also at low *real* frequencies $\omega \ll \Omega_i$, the Hall conductivity is still important when $\nu_i \approx \Omega_i$:

$$\sigma_P \approx \frac{n_e e}{B} \frac{\kappa_i}{1+\kappa_i^2}, \tag{2.24}$$

$$\sigma_H \approx \frac{n_e e}{B} \frac{1}{1+\kappa_i^2}, \tag{2.25}$$

with $\kappa_i = \Omega_i/\nu_i$. Two directions of phase propagation, purely along $\mathbf{B}$, $\mathbf{k}_\perp = 0$, and transverse, $k_z = 0$, will be discussed.

Along $\mathbf{B}$, the Hall effect generates right and left circularly polarized characteristic modes with different skin depths:

$$\delta_\pm = \left(\frac{2}{\nu_0 \omega [(\sigma_p^2 + \sigma_H^2)^{1/2} \pm \sigma_H]} \right)^{1/2}. \tag{2.26}$$

For parallel propagation the left-handed mode propagates deeper than the right-handed into a dissipative plasma; for antiparallel propagation the reverse holds.

For purely transverse propagation, the real phase velocities and the skin depths of both modes are degenerate, and may be written using the Cowling conductivity:

$$k_\perp^2 = i \frac{\omega \nu_i}{v_A^2} = i \mu_0 \omega \left(\sigma_P + \frac{\sigma_H^2}{\sigma_P} \right); \tag{2.27}$$

this mode is heavily damped.

Of course, our results so far are not completely new. For metals and semiconductors, an early references seems to be Miller (1961), who obtained the refractive index for parallel propagating circularly polarized waves in a form similar to (2.18), but including the displacement current. Papadopoulos *et al.* (1994) again considered parallel propagation only in a plasma with ion–neutral collisions. They proposed to use the name 'helicon' from solid state physics nomenclature (Platzman and Wolff 1973) for the low-frequency case $\omega < \Omega_i$, and to retain whistler for $\omega > \Omega_i$.

We shall now turn our attention to the Earth's ionosphere, where a strong steady-state Hall effect is known to exist, but whose dynamics so far have essentially been ignored. At low frequencies the vertical atmospheric scale is much smaller than field-parallel wavelengths or skin depths of Alfvén waves. Then wave propagation is best considered as a reflection and transmission process.

3. Reflection of Alfvén waves from a thin ionosphere

The reflection of torsional modes from a boundary to a dissipative plasma with Hall currents is considered in this section. Such a situation occurs for example when Alfvén waves propagating in the mostly non-dissipative space plasma hit the Earth's ionosphere, often in connection with auroral phenomena. A few idealizing assumptions are made.

The time scale for the acceleration of the neutral gas by ion drag is of the order of many hours; it is therefore considered as stationary. Our linear analysis

https://doi.org/10.1017/S0022377897006223 Published online by Cambridge University Press

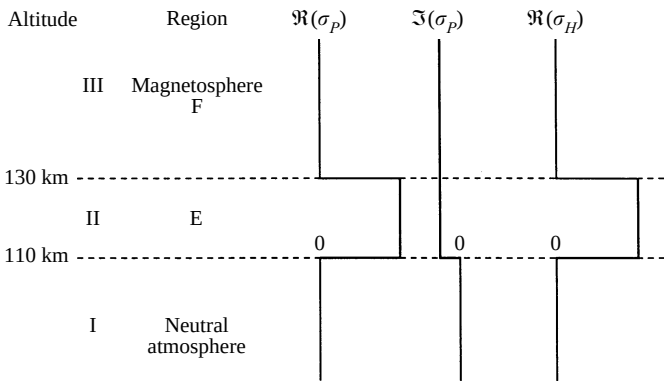


Figure 2. Sketch of the regions for which the reflection of Alfvén waves is considered, with greatly simplified conductivity profiles.

assumes small amplitudes, which is sufficient here, since the geomagnetic field is about 50000 nT, and the observed variations are only a small fraction of this.

Conductivities are assumed to be homogeneous in the horizontal direction. The magnetic field **B** is vertical, which is approximately the case at high latitudes. using typical dayside value of $\sigma_{P,H}$ and v_A in the Earth's ionosphere, at wave periods longer than about 1 s the wavelengths are much larger than the parameter gradients in the vertical direction. Then the stratification may be modelled by three regions (see also Fig. 2):

(I) a natural atmosphere with zero conductivities below about 110 km;

(II) a region with dissipation between about 110 and 130 km, which may be associated with the ionospheric E region; $\sigma_{P,H}$ are approximately real and of the order of 0.1 mS m^{-1};

(III) a region with no dissipation above about 130 km, which may be associated with the ionospheric F region and magnetosphere; there v_A is of the order of 1000 km s^{-1}.

Ω_i is about 300 s^{-1} (for O^+); then the Hall currents are negligible in the F region, but important in the E region owing to frequent ion–neutral collisions. At the frequencies considered, the skin depth of Alfvén waves is much larger than the thickness of the E region (≈ 20 km). Thus the electric field of an Alfvén wave is only slightly attenuated by the dissipation in the E region, although there is a very good conductor ($\Re(\sigma_P) \gg \Im(\sigma_P)$). In fact, electric fields due to auroral activities have been measured using balloons at about 40 km altitude, which is well below the ionosphere. Therefore the fields within the E region are assumed to be independent of z. The influence of the conducting Earth is neglected. This model is rather crude, but will allow us to proceed analytically.

The magnetospheric wave may be decomposed into incident and reflected waves, with vertical wavenumbers k_z and $-k_z$ (in the northern hemisphere both **B** and z are positive downwards), and electric field vectors $\mathbf{E}_I$ and $\mathbf{E}_R$

https://doi.org/10.1017/S0022377897006223 Published online by Cambridge University Press

respectively. The total electric field at the boundary between regions II and III is $\mathbf{E}_I + \mathbf{E}_R$, and the net field-aligned current from (10) is

$$j_\parallel - \frac{i}{\mu_0 v_A} \mathbf{k}_\perp \cdot (\mathbf{E}_I - \mathbf{E}_R). \tag{3.1}$$

Both must be continuous across the boundary.

Neglecting Hall currents throughout, the second term in the large parentheses in (2.23) vanishes. The field-aligned ionospheric current is obtained by integration over region II:

$$j_\parallel = -i\Sigma_P \mathbf{k}_\perp \cdot (\mathbf{E}_I + \mathbf{E}_R), \tag{3.2}$$

where $\Sigma_P = \int_{II} \sigma_P \, dz$ is the height-integrated Pedersen conductivity. Both currents must be equal; then the relation between incident and reflected fields is

$$\mathbf{E}_R = \frac{\Sigma_A - \Sigma_P}{\Sigma_A + \Sigma_P} \mathbf{E}_I, \tag{3.3}$$

where $\Sigma_A = 1/\mu_0 v_A$ is the Alfvén-wave impedance of the magnetosphere. This result was first derived by Scholer (1970) using another method. The problem is similar to that for a transmission line terminated by a resistor.

In order to take account of the ionospheric self-induction due to alternating Hall currents we proceed similarly to calculations of the magneto-optical Kerr effect in solid state physics. The incident wave, which is assumed to be purely torsional in region III, is written as a linear combination of two modes in region II corresponding to the + and − signs in (2.21)–(2.23):

$$\mathbf{E}_I = (a^{(+)} + a^{(-)}) \mathbf{E}_I. \tag{3.4}$$

Of course, $a^{(+)} + a^{(-)} = 1$. The second condition for $a^{(\pm)}$ is that the net incident compressional field vanishes:

$$-\hat{\mathbf{z}} \times \mathbf{E}_C = \left(a^{(+)} \frac{2y_H}{1 + (1 + 4y_H^2)^{1/2}} + a^{(-)} \frac{2y_H}{1 - (1 + 4y_H^2)^{1/2}} \right) \mathbf{E}_I = 0. \tag{3.5}$$

The result is

$$a^{(\pm)} = \frac{2y_H^2}{(1 + 4y_H^2)^{1/2} [(1 + 4y_H^2)^{1/2} \mp 1]}. \tag{3.6}$$

The incident torsional wave excites both characteristic modes in the E region. In order to obtain an approximate result, we assume also that $\sigma_{P,H}$ are independent of z in the E region (and thus so is y_H), and define $\Sigma_{P,H} = \Delta z \, \sigma_{P,H}$. The reflection coefficients for the torsional (irrotational) component of both modes may be calculated completely analogously to the procedure in the paragraph above, namely by applying the conditions of continuity of the electric field and of the field-aligned current:

$$R^{(\pm)} = \frac{[1 \pm (1 + 4y_H^2)^{1/2}] (\Sigma_A - \Sigma_P) + 2iy_H \Sigma_H}{[1 \pm (1 + 4y_H^2)^{1/2}] (\Sigma_A + \Sigma_P) - 2iy_H \Sigma_H}. \tag{3.7}$$

https://doi.org/10.1017/S0022377897006223 Published online by Cambridge University Press

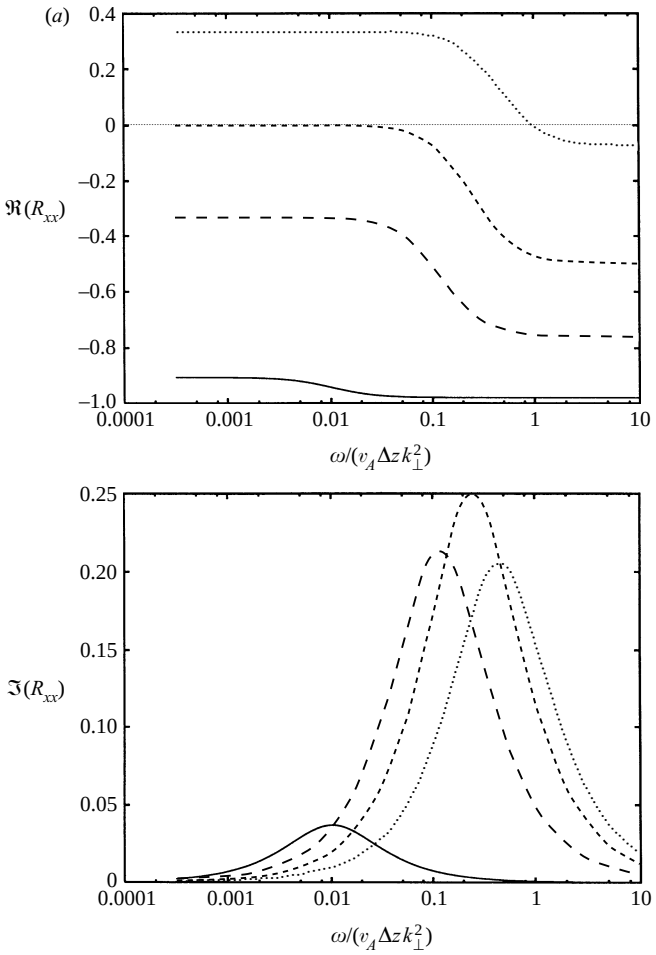


Figure 3(*a*). For caption see facing page.

The diagonal elements of the reflection tensor

$$\mathbf{R} = \begin{pmatrix} R_{xx} & R_{xy} \\ -R_{xy} & R_{xx} \end{pmatrix} \tag{3.8}$$

may be calculated from

$$R_{xx} = a^{(+)} R^{(+)} + a^{(-)} R^{(-)}. \tag{3.9}$$

The reflected field now also has a compressional component, which is related to the reflected torsional field through (2.21). The off-diagonal element is therefore

$$R_{xy} = -2iy_H \left(\frac{1}{1+(1+4y_H^2)^{1/2}} a^{(+)} R^{(+)} + \frac{1}{1-(1+4y_H^2)^{1/2}} a^{(-)} R^{(-)} \right) \tag{3.10}$$

$$= \frac{-iy_H}{(1+4y_H^2)^{1/2}} (R^{(+)} - R^{(-)}). \tag{3.11}$$

https://doi.org/10.1017/S0022377897006223 Published online by Cambridge University Press

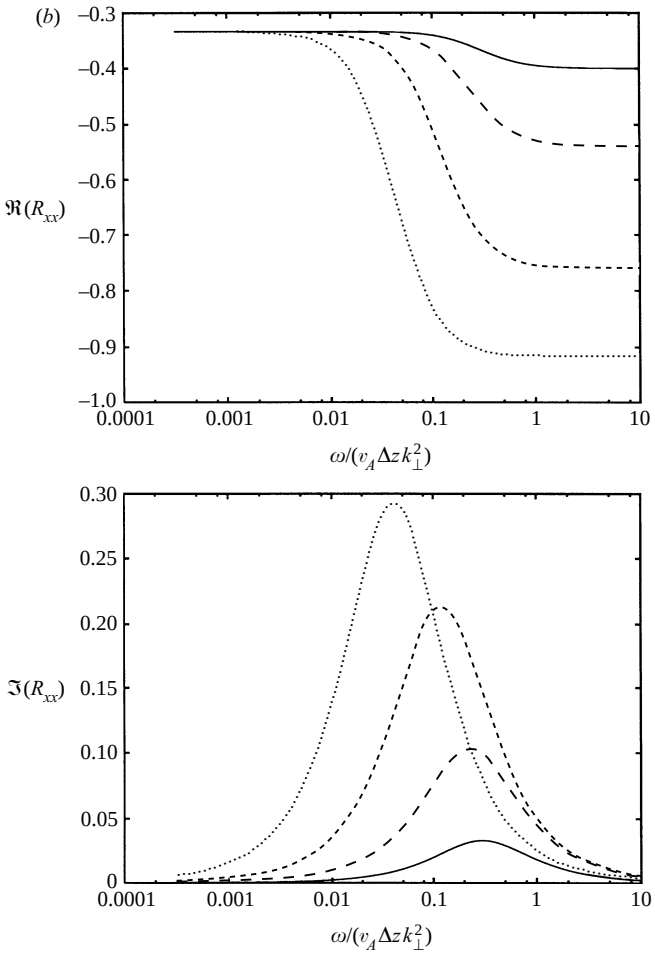


Figure 3. Real and imaginary parts of the diagonal elements of the reflection tensor versus the dimensionless frequency/wavenumber parameter $a = \omega/(v_A \Delta z\, k_\perp^2)$. In (*a*), the magnetospheric Alfvén-wave impedance Σ_A is varied, $\Sigma_P = 2$ S and $\Sigma_H = 4$ S: ——, $\Sigma_A = 0.1$ S; – – –, 1 S; ----, 2 S; . . . . . , 4 S. In (*b*), Σ_H is varied, $\Sigma_P = 2$ S and $\Sigma_A = 1$ S: ——, $\Sigma_H = 1$ S; – – –, 2 S; ----, 4 S; . . . . . , 8 S. Dispersion is most significant when the impedances approximately match, $\Sigma_A \approx \Sigma_P$. The curves with $\Sigma_A = 1$ S, $\Sigma_P = 2$ S and $\Sigma_H = 4$ S should represent quite typical values for an illuminated Earth's ionosphere at high latitudes.

As a final result,

$$\mathbf{E}_R = \mathbf{R}\cdot\mathbf{E}_I, \tag{3.12}$$

$$\mathbf{R} = \frac{1}{N}\begin{pmatrix} P & -H \\ H & P \end{pmatrix}, \tag{3.13}$$

$$N = \Sigma_A(\Sigma_A + \Sigma_P) - ia[(\Sigma_A + \Sigma_P)^2 + \Sigma_H^2], \tag{3.14}$$

$$P = \Sigma_A(\Sigma_A - \Sigma_P) - ia(\Sigma_A^2 - \Sigma_P^2 - \Sigma_H^2), \tag{3.15}$$

$$H = -2ia\Sigma_a\,\Sigma_H, \tag{3.16}$$

$$a = \frac{\omega}{\Delta z\, k_\perp^2\, v_A} \tag{3.17}$$

is obtained.

https://doi.org/10.1017/S0022377897006223 Published online by Cambridge University Press

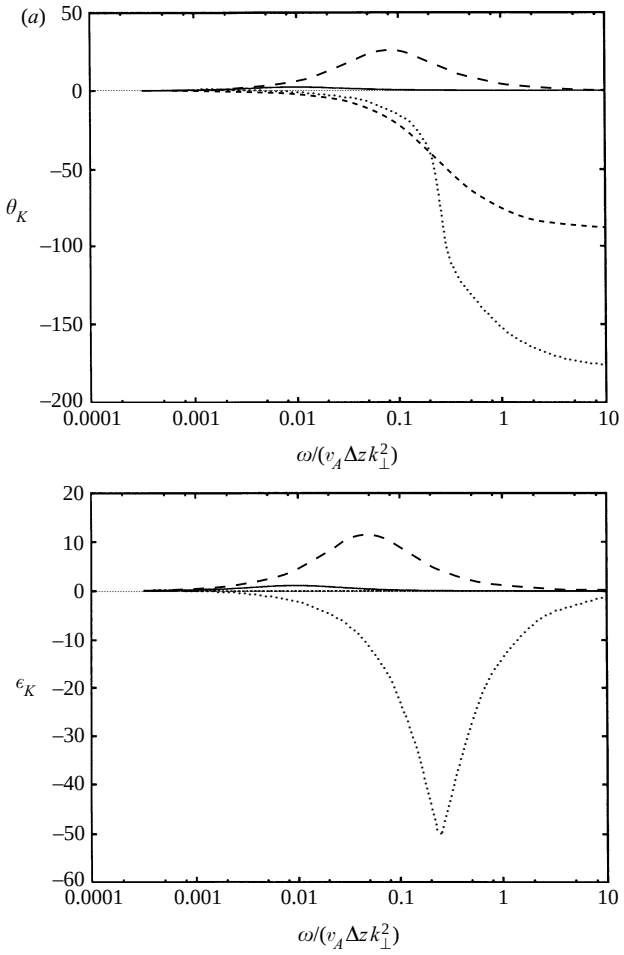


Figure 4(*a*). For caption see facing page.

The reflection tensor becomes diagonal and equivalent to Scholer's result as $\Sigma_H \to 0$ or as the dimensionless parameter $a \to 0$. a is proportional to frequency and inversely proportional to the square of the perpendicular wavenumber. The first condition is physically clear; the second means that the Hall effect is only relevant for wave reflections at sufficiently large wavelengths and frequencies.

Another relatively simple result is obtained in the limit of very high frequencies and large wavelengths $a \gg 1$:

$$R_{xx} = \frac{P}{N} \approx \frac{\Sigma_A^2 - \Sigma_P^2 - \Sigma_H^2}{(\Sigma_A + \Sigma_P)^2 + \Sigma_H^2}, \tag{3.18}$$

$$R_{xy} = -\frac{H}{N} \approx \frac{2\Sigma_A \Sigma_H}{(\Sigma_A + \Sigma_P)^2 + \Sigma_H^2}. \tag{3.19}$$

Between the two limits, when $a \approx 1$, the reflection tensor depends on frequency and wavelength, and is complex even when Σ_P, Σ_H and Σ_A are real and constant. In Fig. 3 the real and imaginary parts of the diagonal elements are plotted.

https://doi.org/10.1017/S0022377897006223 Published online by Cambridge University Press

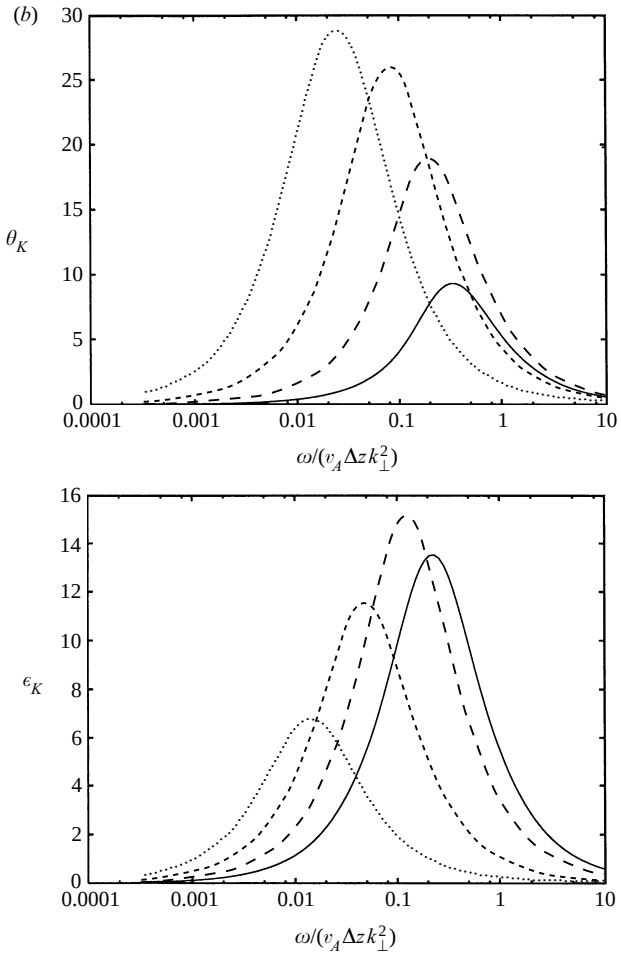


Figure 4. Kerr rotation θ_K and ellipticity ϵ_K versus the dimensionless frequency/wave-number parameter $a = \omega/(v_A \Delta z k_\perp^2)$. In (*a*) the magnetospheric Alfvén-wave impedance Σ_A is varied, $\Sigma_P = 2$ S and $\Sigma_H = 4$ S: ——, $\Sigma_A = 0.1$ S; – – –, 1 S; ----, 2 S; . . . . . , 4 S. In (*b*) Σ_H is varied, $\Sigma_P = 2$ S and $\Sigma_A = 1$ S: ——, $\Sigma_H = 1$ S; – – –, 2 S; ----, 4 S; . . . . . , 8 S. For matching impedances, $\Sigma_A = \Sigma_P$, the reflected wave is purely circularly polarized, $\epsilon_K = 0$, and the value of θ_K is meaningless.

Kramers–Kronig relations, which are of great practical importance in optics, may be verified for the real and imaginary parts of each tensor element (this is also true for the other frequency-dependent factors relating currents and fields in all the equations). The qualitative consequences of these relations are clearly exhibited in Fig. 3; for example, the imaginary part attains a maximum approximately where the derivative of the real part with respect to frequency is a minimum.

The dependence of $k_\perp^2$ indicates that spatial diffusion in the horizontal direction takes place in the reflection. For a wave structure of finite horizontal extent, the reflected wave field is spread relative to the incident wave field.

Locally, if the electric field of the incident wave oscillates in a plane then that of the reflected wave describes an ellipse, which may be derived from the reflection tensor. It is customary to define a Kerr rotation θ_K, which is the angle

https://doi.org/10.1017/S0022377897006223 Published online by Cambridge University Press

between the major axis of the ellipse and the plane of incident polarization, and a Kerr ellipticity ϵ_K, which is the ratio of the minor axis to the major axis of the ellipse. Both angles may be conveniently calculated by decomposing the reflected wave field into right and left circularly polarized parts:

$$r^{(+)} = |r^{(+)}| \exp(i\Delta^{(+)}) = \tfrac{1}{2}(R_{xx} + iR_{xy}), \tag{3.20}$$

$$r^{(-)} = |r^{(-)}| \exp(i\Delta^{(-)}) = \tfrac{1}{2}(R_{xx} - iR_{xy}). \tag{3.21}$$

Then

$$\theta_K = -\tfrac{1}{2}(\Delta^{(+)} + \Delta^{(-)}), \tag{3.22}$$

$$\epsilon_K = \frac{|r^{(+)}| - |r^{(-)}|}{|r^{(+)}| + |r^{(-)}|}. \tag{3.23}$$

In Fig. 4, θ_K and ϵ_K are plotted for different combinations of values for Σ_A, Σ_P, and Σ_H.

Globally, for an incident torsional mode, the reflected wave field derived from the diagonal elements is in the magnetosphere a torsional mode, and the one from the off-diagonal elements is a compressional mode. The latter is evanescent when $k_{z,C}^2 = \omega^2/v_a^2 - k_\perp^2 < 0$, which is the case for most known dynamic phenomena in the auroral ionosphere. This simple argument is due to Hughes (1974). In contrast to the Kerr effect in solid state physics, part of the reflection is a surface wave. The observable polarization of the total electric field will therefore be different between locations close to the surface, the ionosphere and further out in the magnetosphere.

The presence of eddy electric fields driving Pedersen current vortices causes Ohmic heating, and consequences can be expected for the energy flow between magnetosphere and ionosphere. The ratio of the dissipated power per unit area $P = \frac{1}{2}\Sigma_P \mathbf{E}\cdot\mathbf{E}^*$, where $\mathbf{E} = \mathbf{E}_I + \mathbf{E}_R$, and the incident-wave Poynting flux $S_A = \frac{1}{2}\Sigma_A \mathbf{E}_I \cdot \mathbf{E}_I^*$ is maximum when the impedances on both sides of the boundary match. In the case of scalar reflection, (3.1),

$$\frac{P}{S_A} = \frac{4\Sigma_P \Sigma_A}{(\Sigma_A + \Sigma_P)^2}, \tag{3.24}$$

which is maximum when $\Sigma_A = \Sigma_P$. Taking the Hall effect into account,

$$\frac{P}{S_A} = 4\Sigma_P \Sigma_A \frac{\Sigma_A^2 + a^2[(\Sigma_A + \Sigma_P)^2 + \Sigma_H^2]}{\Sigma_A^2(\Sigma_A + \Sigma_P)^2 + a^2[(\Sigma_A + \Sigma_P)^2 + \Sigma_H^2]^2} \tag{3.25}$$

is obtained. This ratio is plotted in Fig. 5. Somewhat unexpectedly, the presence of a Hall conductivity always reduces the amount of energy dissipation compared with an ionosphere that is isotropic. This is due to an increased impedance mismatch. The filter properties of the anisotropic reflection become obvious. For a given wavelength, high-frequency variations bounce off more effectively than the low-frequency ones. For a given frequency, the large-scale wave structures are dissipated more effectively than the small-scale ones. Fourier transformation in time of the reflection tensor (3.12)–(3.17) would give the impulse response tensor of the filter.

https://doi.org/10.1017/S0022377897006223 Published online by Cambridge University Press

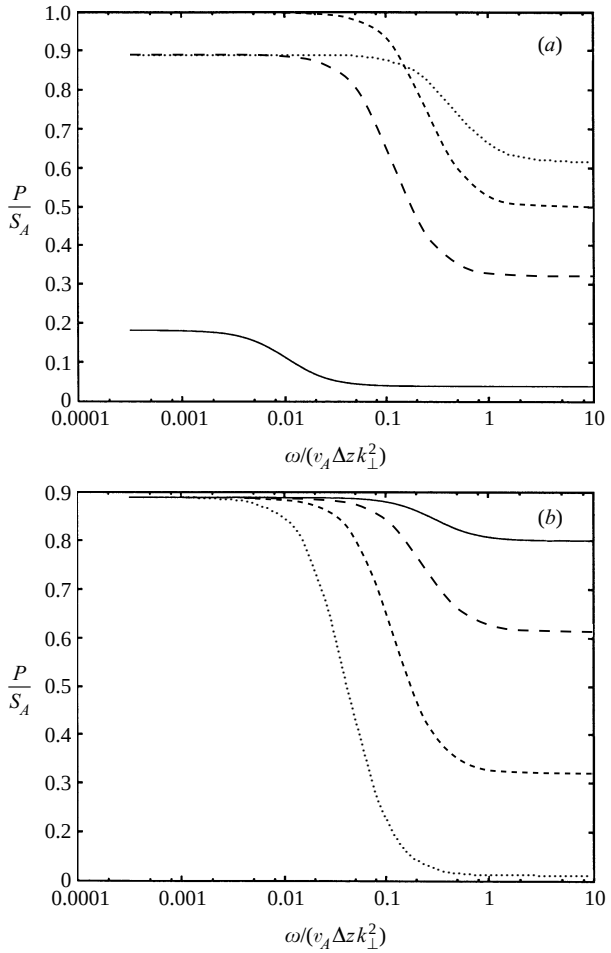


Figure 5. Ratio of energy dissipation per unit ionospheric area and incident-wave Poynting flux versus the dimensionless frequency/wavenumber parameter $a = \omega/(v_A \Delta z\, k_\perp^2)$. In (*a*) the magnetospheric Alfvén-wave conductivity Σ_A is varied, $\Sigma_P = 2$ S and $\Sigma_H = 4$ S: ——, $\Sigma_A = 0.1$ S; – – –, 1 S; - - - -, 2 S; . . . . . , 4 S. In (*b*) Σ_H is varied, $\Sigma_P = 2$ S and $\Sigma_A = 1$ S: ——, $\Sigma_H = 1$ S; – – –, 2 S; - - - -, 4 S; . . . . . , 8 S.

4. Discussion

In most works, self-induction in the Earth's ionosphere has been considered, often implicitly, as unimportant. However, this is not always valid, owing to the very strong Hall effect in the E region. Let us consider horizontal scales of the order of 500 km, which would apply to auroral phenomena such as 'westward-travelling surges' and 'eastward-drifting Ω bands'. Assuming a moderately ionized F region, $v_a \approx 1000$ km s^{-1}. We infer from Figs 3 and 4 that the strongest dispersion and maximum Kerr rotation occurs when $a \approx 0.1$. This is achieved when the horizontal phase velocity $\omega/k_\perp$ is of the order of 10 km s^{-1} which is within the range reported from observations (for example by Pellinen *et al.* 1995). At larger scales, even slower variations produce significant induction. At 2000 km wavelength, a typical period of 5 min is obtained using the same criterion. At smaller scales, typical periods obtained for a significant

https://doi.org/10.1017/S0022377897006223 Published online by Cambridge University Press

Kerr rotation become very short; for example, 0.2 s is obtained for $\lambda_\perp = 50$ km. Thus we may conclude that self-induction in the Earth's ionosphere is mainly significant at large scales exceeding about 500 km.

Such large-scale dynamic structures hardly have the form of linearly polarized plane waves, and the Kerr effect as such is probably difficult to observe directly. However, we predict two main observational consequences. First, over large scales (at least a few hundred kilometres), significant instantaneous eddy electric fields will be measurable in active periods. These could be observed by ground-based coherent and incoherent scattering radars. Secondly, hodograms (traces of the electric field vector) on the same field line are different between the ionosphere and magnetosphere owing to the excitation of the surface waves. Field-line resonances in the ULF range usually show a clear polarization, but for the typical horizontal scale of this phenomenon the predicted differences are relatively small, and the Kerr angle is only a few degrees. If the effect were stronger then the resonance would probably be destroyed. In simulations, where natural noise is absent, the different hodograms could be clearly reproduced (Budnik 1996). In rapidly changing large-scale auroral phenomena the plasma motion measured just above the E region will be greatly distorted compared with the magnetospheric convection. A more detailed modelling of this effect will be published elsewhere.

The simple analytical theory of Alfvén-wave reflection presented here assumes homogeneous regions in space, which is probably unrealistic most of the time for the Earth's ionosphere. Therefore we have not yet compared our results with observations. Ground-based magnetic field measurements, which are available from many observatories, are only sensitive to the source-free horizontal current component, as has been shown by Fukushima (1969). Knowledge of these currents alone, according to our theory, is not sufficient to separate potential and inductive components of the electric field. Further complications can be expected due to strong horizontal gradients of the conductivities, whose effects were modelled by Glassmeier (1984). Thus a combination of field and conductivity measurements from advanced instrumentation will be necessary for an assessment of the dynamics of the Hall effect in the E region. The theory will need to be extended and take into account an inhomogeneous medium. Then the present formulation in Fourier space becomes inconvenient in general, and numerical methods probably need to be applied.

5. Conclusions

The new result of this work is the reflection of Alfvén waves from a magneto-optically active dissipative thin plasma sheet. It is a transformation of one of the most fundamental magneto-optical effects (after the Faraday effect) to plasma physics. Application of these results also to other problems in space and laboratory plasmas will be possible.

The ionosphere is one of the major sinks of energy and momentum in the magnetosphere, but many details of the coupling processes involved are still not understood. We have shown that the energy transfer is highly dependent on time and spatial scales. The ionosphere has been termed a brake for magnetospheric convection. In dynamic situations a more precise technical

https://doi.org/10.1017/S0022377897006223 Published online by Cambridge University Press

analogy is the eddy-current brake. It turns out to be less effective here than the ordinary brake. Induction electric fields at the Earth's magnetospheric footprints are predicted to be present and significant. Further consequences for feedback mechanisms between ionosphere and magnetosphere need to be investigated – this is only a first step.

References

Budnik F. 1996 Numerische Simulationen zum Einfluß der Ionosphäre auf MHD-Wellen in einer Dipolmagnetosphäre. Diploma Thesis, TU Braunschweig.

Chapman, S. and Cowling, T. G. 1939 *The Mathematical Theory of Non-Uniform Gases*. Cambridge University Press.

Dungey, J. W. 1962 Hydromagnetic waves and the ionosphere. *Proceedings of Conference on the Ionosphere*, pp. 230–232. Institute of Physics, London.

Fukushima, N. 1969 Equivalence in ground geomagnetic effect of Chapman–Vestine's and Birkeland–Alfvén's electric current systems for polar magnetic storms. *Rep. Ionos. Space Res. Japan* **23**, 219–227.

Glassmeier, K.-H. 1984 On the influence of ionospheres with non-uniform conductivity distribution on hydromagnetic waves. *J. Geophys.* **54**, 125–137.

Glassmeier, K.-H. 1995 ULF pulsations. *Handbook of Atmospheric Electrodynamics*, pp. 463–502. CRC Press, Boca Raton, FL.

Hasegawa, A. and Uberoi, C. 1982 *The Alfvén Wave*. National Technical Information Service, Springfield, VA.

Holter, Ø. and Kildal, A. 1973 Waves in plasmas. *Cosmical Geophysics* (ed. A. Egeland, Ø. Holter and A. Omholt), pp. 247–265. Universitetsforlaget.

Hughes, W. J. 1974 The effect of the atmosphere and ionosphere on long period magnetospheric micropulsations. *Planet. Space Sci.* **22**, 1157–1172.

Kan, J. R., Zhu, L., Lui, A. T. Y. and Akasofu, S.-I. 1991 A magnetosphere–ionosphere coupling theory of substorms including magnetotail dynamics. *Auroral Physics* (ed. C.-I. Meng, M. J. Rycroft and L. A. Frank), pp. 312–321. Cambridge University Press.

Miller, P. B. 1961 Frequency-dependent Hall effect in normal and superconducting metals. *Phys. Rev.* **121**, 435–450.

Papadopoulos, K., Zhou, H.-B. and Sharma, A. S. 1994 The role of helicons in magnetospheric and ionospheric physics. *Comments Plasma Phys. Contr. Fusion* **15**, 321–337.

Pellinen, R. J., Pulkkinen, T. I., Huuskonen, A. and Glassmeier, K.-H. 1995 On the dynamical development of the downward field-aligned current in the substorm current wedge. *J. Geophys. Res.* **100**, 14 863–14 873.

Platzman, P. M. and Wolff, P. A. 1973 *Waves and Interactions in Solid State Plasmas*. Academic Press, New York.

Prange, R., Rego, D., Southwood, D., Zarka, P., Miller, S. and Ip, W. 1996 Rapid energy dissipation and variability of the Io–Jupiter electrodynamic circuit. *Nature* **379**, 323–325.

Reim, W. and Schoenes, J. 1990 Magneto-optical spectroscopy of f-electron systems. *Ferromagnetic Materials*, Vol. 5 (ed. K. H. J. Buschow and E. P. Wohlfarth), pp. 133–236. Elsevier, Amsterdam.

Scholer, M. 1970 On the motion of artificial ion clouds in the magnetosphere. *Planet. Space Sci.* **18**, 977–1004.

Stix, T. H. 1962 *The Theory of Plasma Waves*. McGraw-Hill, New York.

https://doi.org/10.1017/S0022377897006223 Published online by Cambridge University Press